DE-NEUTRALIZATION OF LASER PRODUCED PROTON PULSE IN A STRONG SOLENOIDAL MAGNETIC FIELD

M. Droba, O.Kester, O. Meusel, C. Wiesner, Institut fuer Angewandte Physik, Goethe University, Frankfurt am Main, Germany.

Abstract

Laser generated proton pulses of ten to several ten MeV produced in PHELIX-laser facility at GSI Darmstadt possess some unique characteristics. The first systematic exploration of the interface between proton pulse generation via the TNSA mechanism and conventional accelerator technology is within the scope of the LIGHT (Laser Ion Generation, Handling and Transport) project. One of the main tasks is to study the beam dynamics in intense B-fields, especially in context of early de-neutralization and space charge effects. 3D numerical simulations with co-moving electrons and up to 10^7 macroparticles were performed to investigate the de-neutralization process in the focusing magnetic solenoid. The Importance of the first focusing element and influence on beam parameters will be addressed. Results of the 3D simulation model will be presented and discussed.

INTRODUCTION

The proton pulses generated by intense Laser pulses (via Target normal sheet acceleration (TNSA)[1] and Radiation Pressure Acceleration (RPA)[2] techniques) seem attractive for further consideration as a new pulsed particle source especially due to the generated high particles number ($N \sim 10^{13}$), very small emittance values (in a range of 1πmm mrad) and small dimensions (few tens of μm) at the production target. For a successful manipulation of the proton pulse parameters after generation it is necessary to expand the pulse in transversal and longitudinal dimensions. This situation can be compared to the initial stage of the high current accelerator schemes with an ion source, extraction system and LEBT (Low Energy Beam Transport) section with an aim of a beam preparation with a minimum emittance growth. However, the proton pulse exhibits unique characteristics like energy spectrum, energy dependent opening angles, radii and pulse structure. Also the co-moving electrons take an influence on the pulse propagation.

In previous papers [3, 4] a beam transport study through the strong pulsed magnetic solenoid, chosen as a first focusing element and an injection in a post-acceleration structure was presented. The simplified transport with co-moving electrons (their influence on the proton pulse was neglected after 460ps mainly due to the run time of the simulation and expanded pulse dimensions with relaxing space charge forces) led to the accumulation of the proton fraction on axis.

This work is focused on a completed simulation campaign (with the same parameter settings as in [3, 4]), comparison with the results of a simplified model and electron column dynamic inside of a strong solenoidal magnetic field.

SIMULATION PARAMETERS

The initial proton pulse characteristics have been discussed in Ref. [3, 4] in detail and main parameters are listed in Table 1.

Table 1: Initial Parameters

Parameter	
Type of distribution	Gaussian 2σ
Spectral interval	5-15MeV
Initial radius	from 280 μm at 5 MeV to 70 μm at 15 MeV
Angular divergence	400 – 140 mrad
Start length of the pulse	22μm

Preliminary simulation checks resulted in an optimum cylindrical mesh setting. (Δr=4μm, Δz=2μm, Δϕ=0.21rad in time interval 0-30ps, Δr=45μm, Δz=45μm, Δϕ=0.21rad in time interval 30-40ps, Δr=88μm, Δz=88μm, Δϕ=0.21rad in time interval 40ps-3ns). Improved statistics (10^7 macroparticles) was crucial, to cover the space charge shielding effects, species to species momentum transfer and relatively big energy spread. Therefore the simulation required a very long time (more than 5000hours on 50 processors). Special attention was focused on finding an optimum simulation time step Δt in respect to the electron column, which could be spread over a long distance in longitudinal direction. Magnetic and electric field levels are strongly position dependent and hence influence the appropriate time step Δt.

DE-NEUTRALIZATION

In the initial stage, the electron column was chosen co-moving and 100% overlapping the proton pulse. In the first 10ps we assumed isothermal expansion, afterwards the proton and electron distributions start to separate due to the fringing field of the magnetic solenoid (maximum field strength |B|=18T). The electrons are confined by the magnetic field, while protons expand transversally driven by their large transversal momenta.

Because of charge separation, the potential energy of the particles is growing. This growth must be

ISBN 978-3-95450-115-1

Copyright © 2012 by IEEE – cc Creative Commons Attribution 3.0 (CC BY 3.0) — cc Creative Commons Attribution 3.0 (CC BY 3.0)

compensated to conform to energy conservation. It was found, that the proton transversal energy is decreasing in the same amount in time interval 10-40ps (see Fig. 1).

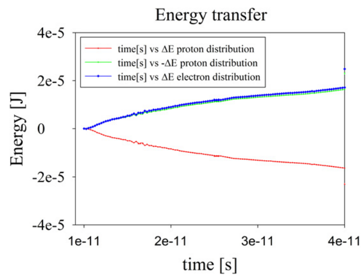

Figure 1: Total energy (potential plus kinetic energy summed over all particles) variation for proton and electron distributions in initial stage of separation.

The on-axis potential accelerates electrons from the pulse along the longitudinal axis in both directions (minimum potential φ=-40kV was reached at t=40ps). After some hundred ps, the electrons are spread around the proton pulse on axis and the potential distribution changed to the form shown in Fig. 2. The situation could be compared with an 1D model of maximum extracted current density by an acceleration gap, known as the Child-Langmuir law [5]. The potential distribution along z-axis is given by

$$\varphi(z) = \varphi(z_0) - \left(\varphi(z_0)^{\frac{3}{4}} - \frac{3}{2}\sqrt{k} \cdot (z - z_1) \right)^{\frac{4}{3}} \quad (1)$$

, where $\varphi(z_1)=0$ and k is a constant proportional to the current. As seen on Fig. 2 (down) the potential distribution is well fitted (red curve) by the equation (1) globally, while the potential distribution in the region of the proton pulse itself differs. The potential acts attractive for electrons in that area and forms a local trap together with longitudinal magnetic field.

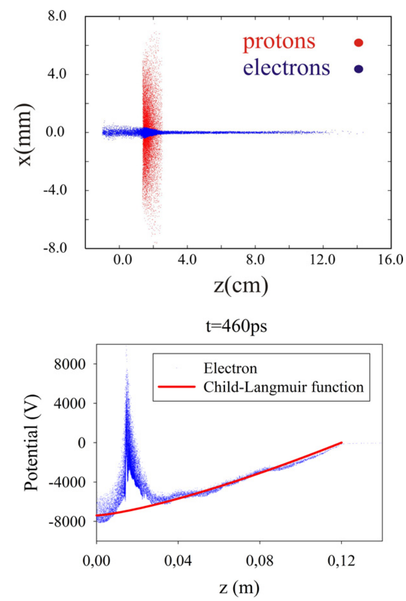

Figure 2: (up) Particles distribution at propagating time t=460ps, (down) potential distribution as seen by electrons at same time.

The confined electron column showed a hollow transversal profile formed by the outgoing electron flow in first 40ps. The evolution of transversal electron distribution in later stage is shown in Fig. 3. Various rotational modes appear in the simulation. The influence on the proton distribution however will be time averaged because of rapid E×B rotation. The confined electron column causes a continuous electrostatic focusing force on axis and its strength was compared with focusing properties of solenoid. This is demonstrated by showing angular frequencies ω_c and ω_{ExB} for the protons along the longitudinal axis in Fig.4. In the first 2cm the electrostatic focusing dominates and protons are accumulated on the axis. In the cross over point the condition of rigid rotor is fulfilled. Afterwards the solenoidal focusing prevails and no more proton accumulation on axis is possible.

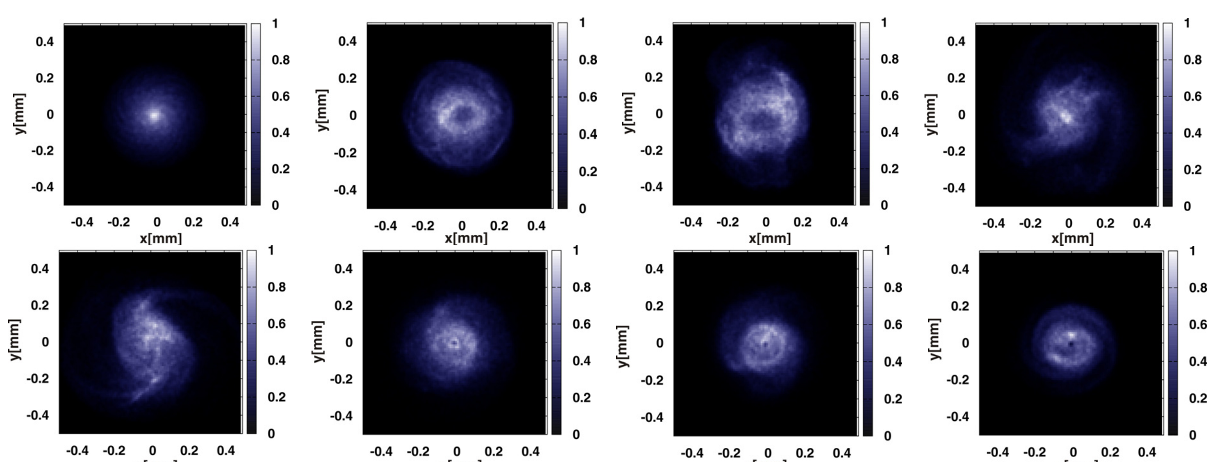

Figure 3: Evolution of the transversal electron column confined with an intense proton pulse in a solenoidal magnetic field.

Copyright © 2012 by IEEE – cc Creative Commons Attribution 3.0 (CC BY 3.0) — cc Creative Commons Attribution 3.0 (CC BY 3.0)

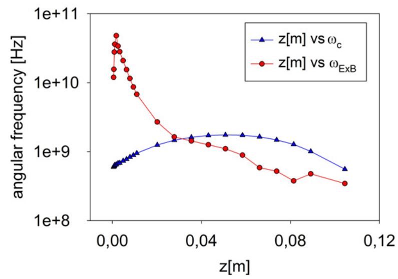

Figure 4: Angular frequencies ω_c and ω_{ExB} for the protons along the longitudinal axis. The protons are accumulated on axis mainly in the first few cm near the target, where ω_{ExB} dominates over ω_c.

The spectral distribution of the electron column is heated, with a peak around 4keV, which corresponds to the co-moving electron energy. The hot electrons are leaving the potential trap of the proton pulse. The energy spread decreases (see Fig. 5) with propagating time.

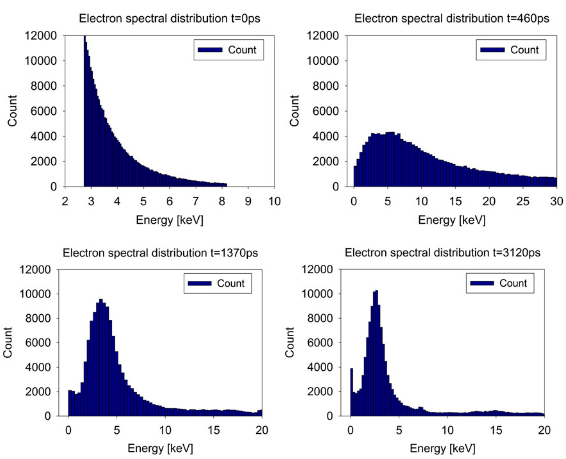

Figure 5: The spectral distribution of electron column

One of the main tasks in this work was approving the simplified model in Ref. [4], where the influence of co-moving electrons was neglected after 460ps. The comparison between simplified model (Sim A) and complete transport (Sim B) for the whole proton pulse in phase space is shown in Fig. 6.

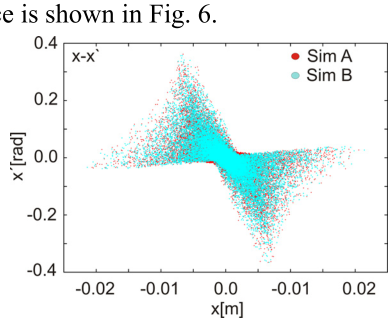

Figure 6: Phase space distribution through the whole proton energy spectrum at time t=3.1 ns.

Very good agreement was achieved with only minor changes. The phase space proton distribution near the axis starts defocusing in Sim A immediately after neglecting electrons, while in Sim B the confining fields are still present.

COMPARISON WITH LEBT

The situation with laser generated proton pulses and co-moving electrons can be compared with LEBTs for high current applications. Here the beam potential confines compensation electrons and charge separation due to the focusing solenoidal magnetic field occurs in the same way. However, the dynamics are not in the highly transient regime as in the laser generated case and all processes are slower. The electron dynamics for such scenarios could be studied in simple way as shown in Fig. 7.

Here a simple optical diagnostic system was used to record the transversal electron dynamics confined in a beam potential and a solenoidal magnetic field.

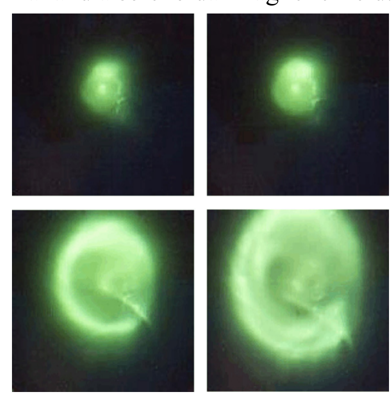

Figure 7: The optical diagnostics of compensation electrons confined in He^{+} (W=14keV, I=2.3mA) beam and solenoidal magnetic field.

CONCLUSION AND OUTLOOK

The investigation of dynamical processes in high current beams and pulses in presence of compensation electrons is crucial for optimisation of future accelerators. Simulations on massive parallel architectures and experimental measurements can help to improve the description for two species transport. First results are very promising and will be used for simulations under different conditions.

REFERENCES

[1] H. Schwoerer et al., Nature 439, 445 (2006).
[2] X.Q. Yan, et al., Phys. Rev. Letters 103(2009) 135001-1.
[3] A. Almomani et al., Proceeding of IPAC'11, San Sebastian, Spain, WEPS033, p. 2556 (2011); http://www.JACoW.org.
[4] A. Almomani, M. Droba, I. Hofmann, U. Ratzinger, Phys. Rev. ST Accel. Beams(to be published)
[5] C.D. Child, Phys. Rev. (Series I) 32, 492–511 (1911).

Copyright © 2012 by IEEE – cc Creative Commons Attribution 3.0 (CC BY 3.0) — cc Creative Commons Attribution 3.0 (CC BY 3.0)